IRJIEST 11, 2025 41 - 51
Available online at https://ojs.batstate-u.edu.ph
International Research Journal on Innovations in Engineering, Science and Technology

Computational fluid design and structural simulation of a corrosion-resistant high-pressure curing vessel for continuous salted egg processing

Allan B. De Villa[a,*], Gerald T. Aguila[a], Mary Rose F. Persincula[b], Rhonalyn V. Maulion[b]

[a]*Department of Mechanical Engineering, College of Engineering, Alangilan Campus, Batangas State University, The National Engineering University, Batangas City 4200, Philippines*

[b]*Department of Chemical Engineering, College of Engineering, Alangilan Campus, Batangas State University, The National Engineering University, Batangas City 4200, Philippines*

ABSTRACT

The design of a rapid, hygienic curing vessel for continuous salted-egg production requires a system that can maintain high pressure, uniform thermal flow, minimal internal flow, and long-term corrosion resistance to highly saline and acidic environments. This study used computational fluid dynamics (CFD), finite element analysis (FEA) and thermal modelling to evaluate a curing vessel with a capacity of 15,360-egg and is made up of AISI 1020 cold-rolled steel Static structural analysis under operating conditions of 404 kPa and 60°C has achieved a maximum von Mises stress of 2.207×10^8 N/m and a Factor of Safety of ≈1.59 with material yield strength of 3.5×10^8 N/m². CFD simulations using the properties of brine showed a bulk average velocity of ~0.01 m/s, near-zero mass flow rate (–0.0002 kg/s), and pressure variation below 1 kPa, which confirms a quiescent and diffusion-dominated environment that is essential for uniform salt penetration. Thermal analysis demonstrated temperature uniformity within ±1°C across the 293–353 K. To address the effect of long- term corrosion risks, the vessel design used a food-grade thermoset epoxy coating with a PVDF liner. The simulations achieved a thermally stable and corrosion-resistant curing vessel, which is suitable for rapid, continuous salted-egg processing.

***Keywords*:** curing vessel, corrosion, high pressure, simulation, modelling

Received: October 7, 2025 **Revised:** December 17, 2025 **Accepted:** December 23, 2025

1. Introduction

Salted egg making is a 1,400-year-old preservation technique for eggs through smearing a mixture of water, salt, and clay on the eggs or by immersing the egg in saturated brine solution. This traditional process requires 14 to 30 days of curing time and has a variable environmental condition with empirically fabricated equipment, which requires more rapid, hygienic, and high-pressure curing technologies. Recent studies have used microbial inactivation and rapid processes such as mild heat treatments that are enhanced by moderate electric fields that significantly improve decontamination efficiency against E. coli K12 [1] and have ultrasonic-pulsed pressure systems that elevate salt penetration at 120–160 kPa range [2]. These technologies demonstrated improved sanitation and shortened curing cycles, but still require a controlled high-pressure and thermally stable vessel that is capable of ensuring uniform process conditions even for larger production volumes. Despite the advancements in microbial inactivation and process acceleration, the existing literature does not present a curing vessel that is designed to perform sterilization, ozonation, high-pressure curing, corrosion resistance, uniform flow, and thermal distribution within a single integrated system. This absence represents a critical gap in both local and international literature, as high-capacity salted-egg operations still rely on empirically fabricated vessels with limited scientific validation of internal fluid dynamics, structural behavior, and long-term material performance.

To address this gap, this study establishes the need for a simulation model of the curing vessel that is capable of maintaining uniform temperature, pressure stability, minimal flow disturbances, and resistance to highly saline and acidic environments over extended operating periods. The study evaluates whether a multi-physics design framework using CFD, thermal analysis, and structural simulation can effectively identify a vessel geometry and lining configuration that is capable of minimizing stress, deformation, and thermal non-uniformities while ensuring a consistent curing condition for large production of eggs. This objective requires a clearly defined process and structural performance targets which include near-quiescent flow to support diffusion-driven salt penetration, spatial temperature uniformity within ±1°C across an operating range of 293–353 K. Structurally, the vessel must maintain von Mises stress below the yield strength of AISI 1020 cold-rolled steel ($\sigma_{yield} = 3.5 \times 10^8$ N/m²) and capability to limit deformation to ensure a safe and stable operation. Ensuring a long-term corrosion resistance is vital to the curing process of salted egg due to its long exposure to a highly saline brine and ozone environment. Protective linings such as food-grade thermoset epoxy or polymeric barriers like glass-flake coatings are widely recognized for their durability in saltwater environments that often reach service lives of up to 30 years [3-5].

*Corresponding author
Email address: allan.devilla@g.batstate-u.edu.ph

Existing curing vessels are largely constructed based on empirical practice and do not undergo rigorous scientific evaluation to verify their structural performance and characterize their internal flow behavior. Given this limitation, no engineered curing vessel has yet been developed that simultaneously satisfies the demands of a high -pressure operation, thermal uniformity, corrosion resistance, and controlled flow behavior, which is necessary for a consistent and scalable salted-egg production. To bridge the gap, the present study used a numerical method using Finite Element Analysis (FEA) and Computational Fluid Dynamics (CFD) to systematically evaluate stress distribution, deformation, heat transfer, and flow behavior to ensure that the proposed vessel meets the industrial standards for pressure integrity, thermal stability, and curing uniformity. SolidWorks simulations using numerical solvers such as the Jacobi method allow combined mechanical, thermal, and fluid dynamic analysis that is anchored to the material database in the software. This transition from food-processing requirements to multi-physics simulation provides the engineering foundation of the vessel's design for evaluation of stress, thermal gradients, and internal flow patterns in the vessel prior to its fabrication. This approach advances the study on salted-egg production by the use of computational design and optimization, which are not previously covered. The development of a curing vessel using a simulation-driven framework bridges the gap in the existing literature by offering an evidence-based methodology for designing a food -processing pressure vessel that is capable of operating under high-pressure, corrosive, and thermally sensitive environments.

2. Materials and methods

In the design and simulation of a curing vessel for salted eggs, this study established a set of predefined assumptions and design considerations that established the framework for the analysis. The analysis is based on a three-dimensional geometric model of the curing vessel that is characterized by a solid body defined using the Cut-Extrude feature that has specific volumetric properties such as solid body mass (4,184.24 kg), volume (0.53167 m^3), density (7,870 kg/m^3), and weight (41,005.6 N).

The material of construction is assumed to be a cold-rolled AISI 1020 Steel that is modeled as a linear elastic isotropic material. The static simulation used specific loading conditions to simulate the operational environment with a static pressure of 404 kPa (404,000 N/m^2) that is applied as a normal force to two defined faces of the vessel and an operating temperature load of 60°C. The static simulation used fixed geometry constraints that were applied to two faces of the model to analyze the motion of the rigid body and structural supports. The simulations utilize the FFEPlus solve with study name (404-60) based on static analysis, at solid mesh type, with thermal effect that includes temperature loads at zero strain temperature of 298 K, with fluid pressure effects with no soft spring, no in-plane effect, no inertial relief, at automatic incompatible bonding options, with no large displacement, with friction for the free body forces computation, with no friction and with no use of adaptive method.

The flow simulation relied on fluid and brine solution properties and boundary conditions, with working conditions set at a pressure of 404 kPa and a temperature of 60°C. The brine solution has a density of 1200 kg/m³ (for a near-saturated solution), viscosity at approximately $1.5x10^{-3}$ Pa·s (at 20°C, increases with concentration), specific heat at approximately 3500 J/(kg·K), and near saturation salt concentration of approximately 26% NaCl by weight. These properties influence the fluid dynamics and heat transfer characteristics within the vessel, and their accurate representation is crucial for the reliability of the flow simulation for salted egg production. The design basis is centered on a curing vessel specifically designed for salted egg production that involves the application of pressure and temperature as simulated through the specified loads in the static analysis and boundary conditions in the flow simulation. The design is evaluated using a combined approach of static structural analysis using FEA, which focused on stress, displacement, and strain distributions within the vessel, and CFD simulation that focused on fluid dynamic parameters such as mass flow rate, velocity fields, pressure distribution, and temperature distribution. A key aspect of the design basis is the recognition of potential corrosion risks that are associated with the curing process. It used specific measures to mitigate corrosion by the application of thermoset epoxy coatings as a liner formulated for direct food contact to provide a barrier between the vessel material and the corrosive environment.

2.1. Static structural analysis

The structural integrity of the proposed curing vessel was analyzed through finite element analysis (FEA) using SolidWorks 2020 (Dassault Systèmes) for 3D modeling, finite element analysis (FEA), and computational fluid dynamics (CFD) setup. All simulations were executed on a computer workstation equipped with the following specifications: Intel® Xeon Processor W-2123 CPU @ 3.90 GHz, 32 PC4-2666 ECC Memory, Windows 10 Pro 64-bit operating system. These specifications ensure sufficient computational capability for handling large solid meshes, thermal-pressure coupling analyses, and multi-physics simulation workflows. The simulation workflow was as follows:

2.1.1. Geometric modeling

A three-dimensional solid model of the curing vessel was developed using SolidWorks software.

2.1.2. Material characterization

The vessel material was specified as AISI 1020 Steel, cold rolled, and characterized as a linear elastic isotropic material. The material was further defined by its yield strength (3.5 × 10^8 N/m^2), tensile strength (4.2 × 10^8 N/m^2), elastic modulus (2.05 × 10^11 N/m^2), Poisson's ratio (0.29), mass density (7,870 kg/m^3), shear modulus (8 × 10^10 N/m^2), and thermal expansion coefficient (1.17 × 10^-5 /K).

2.1.3. Application of loads and boundary conditions

The simulation used various loads and boundary conditions to replicate the operational environment, such as the following: a pressure load of 404 kPa (404,000 N/m^2) applied as a normal force to all selected vessel faces; a thermal load of 60°C applied to the same faces to simulate the operating temperature; and fixed geometry constraints applied to two faces of the model to constrain rigid body motion.

2.1.4. Factor of safety (FOS)

FOS was used to ensure structural reliability under pressurized and thermal operating conditions. For pressure vessels operating at moderate pressure and temperature levels, and subjected to static, non-cyclic loading, an FOS between 1.5 and 2.0 is commonly recommended in preliminary design stages and aligns with typical engineering practice for food-processing equipment made from carbon steel. In this study, a design FOS of 1.5 was adopted as the minimum structural requirement and is justified based on the vessel's classification as a low-to-moderate pressure system, the absence of cyclic or fatigue loading, the use of AISI 1020 steel with well-established mechanical properties, and the inclusion of corrosion-mitigation measures such as thermoset epoxy coating and a proposed PVDF liner.

2.1.5. Mesh generation

The finite element model was discretized using a blended curvature-based meshing algorithm to capture the geometric complexity of the curing vessel. The mesh utilized a maximum element size of 569.56 mm and a minimum element size of 113.912 mm, resulting in 14,530 nodes and 7,015 elements. The mesh quality evaluation focused on the element aspect ratio, in which a value of 1 indicates an ideal element shape. Engineering standards for element ratios typically range between 3 and 5, with no elements exceeding a value of 10. Accordingly, the generated mesh was refined to ensure compliance. The overall mesh contained 0% distorted elements, confirming the integrity of the geometry. A size and growth ratio of 31.8433 was applied to the critical solid body to ensure localized refinement in regions of expected stress concentration.

2.1.6. Solution procedure

The FFEPlus solver was used in the static analysis, configured to include thermal effects with options that included temperature loads and a zero-strain temperature of 298 K.

2.1.7. Post-processing and analysis

Simulation results were post-processed to extract relevant data, including von Mises stress distribution, resultant displacement, and equivalent strain. These data were assessed for the structural integrity of the vessel design.

2.2. Computational fluid dynamics simulation

The fluid dynamic behavior within the curing vessel was simulated using CFD, that is comprised the following steps:

2.2.1. Geometric model

The three-dimensional solid model of the curing vessel, identical to that used in the static analysis, served as the computational domain.

2.2.2. Fluid domain definition

The fluid domain within the vessel was defined and the working fluid was specified as a brine solution. Fluid properties, such as density, viscosity, thermal conductivity, and specific heat capacity, were assigned based on the characteristics of the curing solution.

2.2.3. Boundary condition specification

Appropriate boundary conditions were applied to the computational domain to represent the operating conditions of the curing process. This working pressure was set to 404 kPa and the working temperature to 60°C as relevant boundaries.

2.2.4. Mesh generation

The fluid domain was discretized using a suitable mesh. The mesh type (e.g., structured or unstructured), element size, and mesh density were determined based on the complexity of the geometry and the anticipated flow characteristics. Mesh refinement techniques were employed in regions of high flow gradients to ensure solution accuracy.

2.2.5. Solver configuration

The CFD simulations were performed using a CFD solver. Appropriate turbulence models were selected based on the expected flow regime. Convergence criteria, solution algorithms, and under-relaxation factors were defined to ensure numerical stability and solution accuracy.

2.2.6. Simulation execution and convergence monitoring

The CFD solver was executed, and the solution was iterated until convergence was achieved. Convergence was assessed by monitoring residuals of the governing equations and their key flow parameters, such as mass flow rate, velocity, and pressure.

2.2.7. Post-processing and data extraction

Upon achieving convergence, the simulation results were post-processed to extract relevant fluid dynamic parameters, which include analysis of the mass flow rate, velocity fields, pressure distribution, and temperature distribution within the curing vessel.

To complement the numerical convergence criteria, the statistical indicators such as minimum–maximum ranges, delta values, and average deviations were monitored for all CFD goals. These metrics serve as quantitative measures of the stability of the solution and allow assessment of variability across iterations. Similarly, structural outputs were compared against analytical bounds to evaluate statistical consistency between simulated and expected physical behavior. These statistical evaluations were used to verify the applicability and reliability of the simulation results prior to interpretation.

The selection of the best vessel configuration was carried out using a structured, multi-criteria decision-making procedure based on the design parameter matrix (Table 1) and design goal and criteria (Table 2).

Table 1. Design parameter matrix template

No.	Parameter (Criterion)	Category	Unit	Goal	Weighted Factor (W)
1	Amount of material (volume or mass)	Material or cost	m^3 or kg	Minimize	0.25
2	Factor of safety (FoS)	Safety	unitless	Maximize	0.30
3	Maximum deformation (δ_{max})	Performance	mm	Minimize	0.20
4	Maximum stress (σ_{max})	Performance	MPa	Minimize	0.15
5	Manufacturing complexity/ease	Material/cost	unitless	Minimize	0.10
				TOTAL	1.00

Table 2. Design goal and criteria

Component	Description
Objective	Design a component (e.g., beam, shaft, bracket) that maximizes load-bearing capacity while minimizing cost
Constraint 1	The maximum allowable stress must be less than the material yield strength ($\sigma_{max} < \sigma_y$)
Constraint 2	Maximum allowable deflection (deformation) must be less than a specified limit ($\delta_{max} \leq \delta_{limit}$)
Constraint 3	Must fit within a defined envelope (size/volume limit).

This matrix evaluates each design alternative against weighted engineering criteria to ensure that the final selection satisfies the curing vessel performance, safety, and material-efficiency requirements. The following procedure was implemented:

Define the evaluation criteria and corresponding weighting factors. Five parameters were identified as critical to pressure-vessel performance, such as FOS, maximum deformation (δ_{max}), maximum stress (σ_{max}), and manufacturing complexity. Each parameter was assigned a weighted factor to normalize the values to equal 1.00 that reflects priorities for safety, performance, and cost.

Establish design goals and constraints. The objective of the design is to maximize load-bearing capacity while minimizing material usage and fabrication cost. Three constraints were imposed: (a) the maximum stress must remain below the material yield strength ($\sigma_{max} < \sigma_y$), (b) deformation must not exceed the allowable limit, and (c) the design must fit within the allowable geometric envelope.

Assign scoring values to each design alternative. Each vessel model was evaluated on a 1–5 scale for every parameter, where 5 represents the most favorable result relative to the design goal. Quantitative simulation outputs such as FOS, σ_{max}, deformation, and total mass were normalized and mapped to the scoring scale to ensure objective assessment across all alternatives. For each model, the assigned score in every criterion was multiplied by its corresponding weighted factor (W). This allowed each design parameter to contribute proportionally to the overall evaluation according to its engineering relevance.

Select the design with the highest weighted performance index that satisfies all constraints. The vessel configuration with the greatest total weighted score and full compliance with structural and geometric requirements was identified as the optimal design. This procedure ensures that the selected model achieves the best balance of safety, stiffness, material efficiency, and fabrication practicality.

This simulation approach covered both static structural analysis and CFD simulations that provided a comprehensive evaluation of the proposed curing vessel design which enabled assessment of both its structural integrity and fluid dynamic performance under representative operating conditions.

3. Results and discussion

The simulation-driven evaluation of the proposed high-pressure curing vessel provides integrated insight into its structural response, thermal behavior, and internal flow characteristics under the specified operating conditions. Instead of presenting the structural, thermal, flow, and corrosion findings separately, this section integrates the outcomes of the finite element structural analysis, computational fluid dynamics (CFD) simulations, thermal assessment, and corrosion-resistance evaluation to provide a comprehensive interpretation of the vessel's performance and its relevance to existing engineering studies.

3.1. Structural performance and material considerations

The three-dimensional configuration of the designed curing vessel for salted-egg processing, as presented in Figure 1, consists of a horizontal cylindrical shell with dished heads, flanged manways for product loading and unloading, and dedicated inlet and outlet nozzles to support brine circulation, venting, and instrumentation. Its internal volume of 0.53167 m^3 is sized to enable high-capacity curing while maintaining a compact footprint suitable for integration into standard food-processing layouts. The external geometry is engineered to support uniform thermal loading, proper insulation placement, and ease of maintenance. This configuration establishes the physical basis for the subsequent structural and CFD simulations used to evaluate pressure containment, flow behavior, and thermal performance under operating conditions.

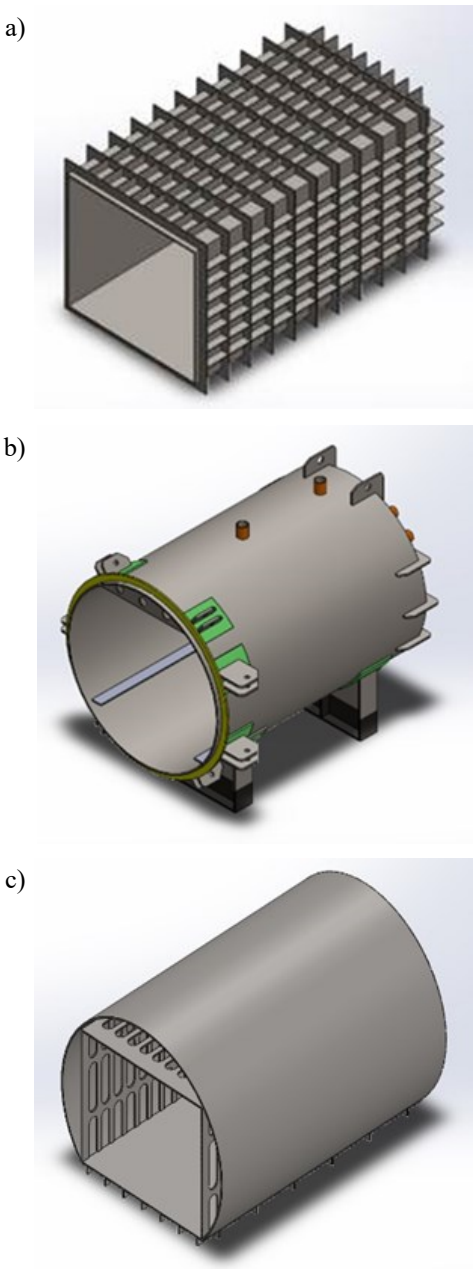

Figure 1. Selected curing vessel geometry (a) Model 1, square, highly ribbed structure; (b) Model 2, robust cylindrical; (c) Model 3, internally ribbed cylindrical structure.

Material selection plays a critical role in ensuring vessel integrity under saline, acidic, and pressurized environments typical of salted-egg curing. AISI 1020 Cold Rolled Steel was selected due to its structural adequacy, with a documented yield strength of 3.5×10^8 N/m² and tensile strength of 4.2×10^8 N/m² [6]. The integration of a corrosion-mitigation system—comprising an FDA-compliant thermoset epoxy coating (21 CFR 175.300) [7] and optional HDPE or PFA polymeric liners [8], which address long-term durability concerns often cited in food-processing vessel design literature. Simulations reveal that the maximum von Mises stress (2.207×10^8 N/m²) remains below the steel's yield strength, confirming elastic behavior and demonstrating that the vessel can safely withstand the applied pressure load of 404 kPa and thermal load of 60°C. The maximum deformation of 2.999 mm falls within acceptable limits for cylindrical pressure vessels, aligning with stress–strain responses reported in similar computational evaluations of food-processing vessels [6].

While these results demonstrate structural suitability, it must be noted that the analysis is linear static; thus, dynamic loading, fatigue effects, weld discontinuities, liner delamination, and corrosion-induced pitting—conditions highlighted in comparable engineering assessments—are beyond the scope of this simulation.

3.2. Comparative assessment of vessel configuration

To ensure that the selected curing vessel geometry represented the optimal configuration for high-pressure salted -egg processing, three design options were subjected to the same structural loading conditions of 404 kPa and 60 °C. The comparative results of the 3 Models were summarized in Table 3. Model 1 (Figure 1a) is geometrically a square vessel reinforced by extensive internal and external ribbing. It is constructed using AISI 1020 Cold Rolled Steel, which has a yield strength of 350.0 MPa, and the mass of the completed structure is 2,959.78 kg.

Table 3. Engineering data for comparative analysis of three (3) Models

Parameter	Unit	Model 1 (Square Ribbed)	Model 2 (Cylindrical)	Model 3 (Cylindrical Ribbed)
Mass (m)	Kg	2,959.78	4,184.24	2,990.53
Yield strength (σ_y)	MPa	350.0	350.0	351.57
Max Von Mises stress (σ_{max})	MPa	468.0 MPa	220.7 399.9	1,669
Max deformation (δ_{max})	mm	7.202 mm	2.999	26.07
Factor of safety (FoS)	unitless	0.748	1.586	0.211

Despite its complexity and heavy ribbing, the square geometry configuration and resultant stress concentrations under the critical 404 kPa load led to a failure. The maximum stress (σ_{max} of 468.0 MPa far exceeded the material's yield strength, resulting in a low FoS of δ_{max} 0.748 and a high

maximum deformation of 7.202 mm, which led the model to be structurally unacceptable for this load case.

Model 2 (Figure 1b) features a robust, simpler cylindrical shape configuration with external mounting features and supports with a yield strength (σ_y) of 350.0 MPa. The cylindrical shape is inherently efficient at handling internal pressure, with a mass of 4,184.24 kg generally heavier than the Model 1. This investment in material provides superior structural performance with a maximum stress δ_{max} of 220.7 MPa and resulted in a high and safe FoS of 1.586. Furthermore, Model 2 demonstrated the best functional stability with the lowest maximum deformation δ_{max} of only 2.999 mm.

Model 3 (Figure 1c) is defined by a semi-circular cylindrical exterior shell supported by an extensive internal ribbed framework with a yield strength (σ_y) of 351.57 MPa. This design is lighter than the other 2 models with 2,990.53 kg mass, but this material efficiency comes at the cost of structural integrity under the high load. The highly concentrated stresses resulting in σ_{max} = 1,669 MPa caused a severe failure with an FoS of only 0.211. This structural instability is evidenced by the massive δ_{max} of 26.07 mm. The results obtained suggested that Model 3 is structurally non-viable.

3.3. Design parameters and weighting

A complete evaluation matrix incorporates three principal categories: performance, material cost, and safety. Each criterion is rated on a numerical scale from 1 to 5, with 5 representing the most favorable outcome, and is assigned a corresponding weighted factor such that the total contribution sums to 1.0 (or 100%) to reflect standard engineering design priorities. Table 4 shows the scoring of each alternative based on 5 selected parameters. A structured scoring matrix considering material amount (25%), safety (30%), performance (20%), max deformation (20%), max stress (15%), and manufacturability (10%) was used to evaluate the models. Model 2 emerges as the most technically sound configuration, which obtained the highest weighted score of 4.30 and stands out as the only design capable of withstanding the critical pressure–temperature load case. In the constraint that maximizes the safety and structural integrity represented by σ_max and FoS, respectively, Model 2 is the sole configuration in which the maximum von Mises stress (σ_max = 220.7 MPa) remains below the material yield strength (σ_y = 350 MPa) and results in a safe Factor of Safety (FoS = 1.586) that is appropriate for pressure-vessel operation.

Table 4. Scoring of each alternative

Parameter	Weight (W)	Model 1 Score	Model 2 Score	Model 3 Score	Model 1 W.Score	Model 2 W.Score	Model 3 W.Score
1. Material Amount	0.25	3 Moderate	4 Low	5 Very Low	0.75	1.0	1.25
2. Factor of Safety	0.30	4 Good	5 Excellent	2 Low	1.2	1.5	0.6
3. Max Deformation	0.20	3 Acceptable	4 Low def	5 Very low def	0.6	0.8	1.0
4. Max Stress	0.15	4 Low stress	4 Low stress	3 Higher stress	0.6	0.6	0.45
5. Manufacturing Complexity	0.10	4 Simple	4 Simple	1 Very complex	0.4	0.4	0.1
Total Weighted Score (Max 5.0)	1.0				3.55	4.3	3.4

In comparison, Models 1 and 3 both exhibited stress levels far exceeding the yield limit with corresponding FoS of 0.748 and 0.211, respectively, which indicate structural failure and permanent deformation under the same operating conditions. Beyond stress performance under criterion 2, Model 2 also provides the most favorable deformation response with a limiting displacement to 2.999 mm that supports dimensional stability throughout operation. The alternative configurations show excessive flexibility deformation in Model 1 (7.202 mm) and Model 3 (26.07 mm), which both exceed acceptable limits for a high-pressure cylindrical vessel. Although Model 2 is the heaviest with 4,184.24 kg, this added material property contributes directly to improved wall stiffness, thickness uniformity, and overall structural stability, which is an acceptable and necessary trade -off given the high weighting assigned to safety and mechanical integrity in the design matrix. Using the structural scoring matrix Model 2, with a total weighted score of 4.25, outperformed Models 1 and 3 in all safety-critical metrics. Only Model 2 met the threshold requirement of FoS 1.0 and deformation within acceptable limits for cylindrical food-processing pressure vessels. Overall, these results confirm that Model 2 is the only configuration that satisfies the fundamental requirement of maintaining a FOS>1.0 under the specified operating conditions. This makes it a sole viable design for continued development and simulation refinement.

3.4. Stress distribution analysis

The static simulation presented in Figure 2 was conducted on the salted egg curing vessel MODEL 2 using SolidWorks simulation to determine the structural integrity under specified operating conditions. The material of the vessel was defined as AISI 1020 Steel, cold rolled, a linear elastic isotropic material with a yield strength of 3.5 x 10^8 N/m^2 and a tensile strength of 4.2 x 10^8 N/m^2. The analysis incorporated a pressure load of 404,000 N/m^2 applied to two

faces, along with a temperature load of 60 degrees Celsius on the same faces. Fixed geometry constraints were applied to specific faces of the model. A solid mesh with blended curvature-based meshing was utilized, resulting in a total of 14,530 nodes and 7,015 elements.

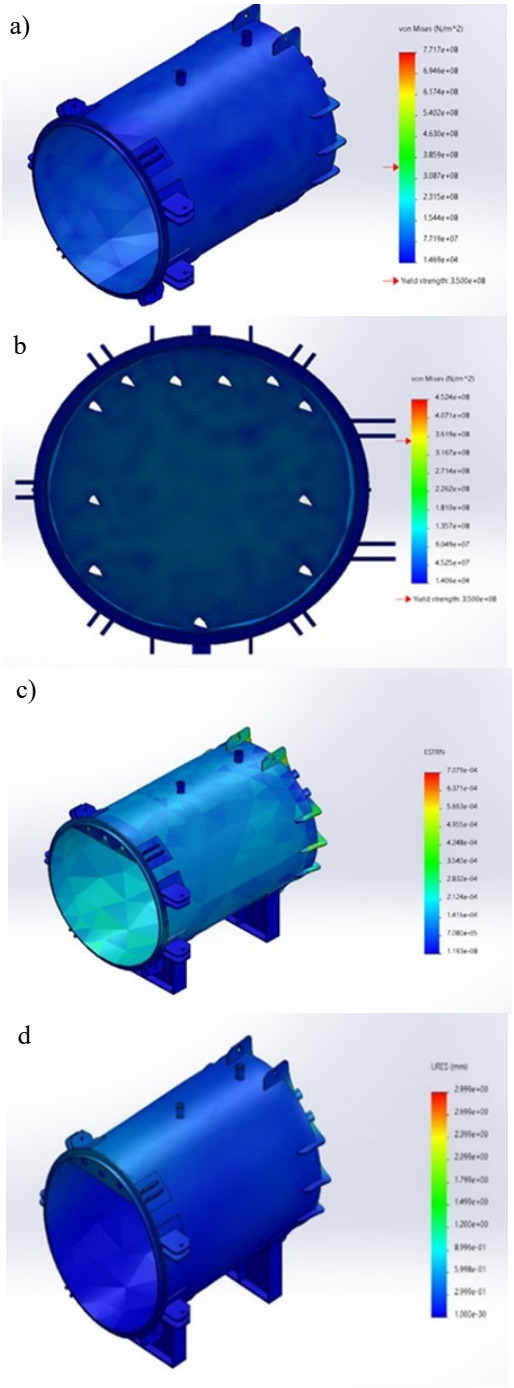

Figure 2. Structural simulation of curing vessels using Solidworks 2020 (a,b) static nodal stress, (c) static stress-strain, and (d) static displacement.

The simulation results revealed a Von Mises stress distribution ranging from 3.916 x 10^3 N/m^2 to 2.207x 10^8 N/m^2. The maximum stress value is below the yield strength of the material, which indicates that the vessel is predicted not to undergo yielding under the applied loads. The displacement ranged from 0.000 mm to 2.999 mm suggested that the current design of the curing vessel has the capacity to withstand the applied pressure and thermal loads without structural failure. However, this analysis is limited to a static simulation only and does not account for the effect of dynamic loads or potential stress concentrations that may occur during corrosion or manufacturing defects. The reliance on linear static analysis introduces inherent limitations consistent with insights from prior pressure-vessel studies, which consider potential discrepancies when cyclic or transient loads are introduced. To ensure the reliability of the model, the current findings should be complemented with prototype testing, fatigue analysis, or transient-thermal stress evaluations in subsequent work.

3.5. Flow behavior and fluid dynamics

3.5.1. Convergence behavior and establishment of quiescence

The convergence behavior of mass flow rate (Figure 3), average velocity, and summary of flow simulation parameters has demonstrated numerical stability across all monitored goals after achieving 100% convergence. The mass flow rate stabilizes near zero or at an average of −0.0002 kg/ which indicates that as the simulation progresses, the fluid motion becomes negligible. This is consistent with the diffusion-dominated curing mechanism as described by Wang et al. [2], which supports the fundamental requirement of minimal convective transport during salted-egg curing. Initial fluctuations in mass flow rate suggest transient thermal and pressure adjustments, which are comparable to those reported in brine-immersion simulations by Chen et al. [9] and diffusion-driven curing optimization studies [10]. The data reveals an initial period of instability, characterized by significant fluctuations. A sharp drop near 50 iterations can be seen in the mass flow rate, which indicates a transient flow behavior during the early iterations. Beyond this initial phase, the mass flow rate converges to a near-zero value at 300 to 500 iterations, which oscillates minimally to around 0 kg/s. This convergence to a negligible mass flow rate substantiates the attainment of a diffusion-dominated process, which is a critical factor for achieving uniform salt penetration in salted egg curing.

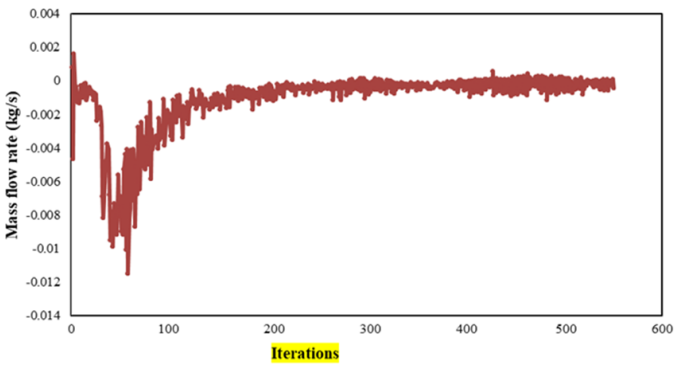

Figure 3. The convergence behavior of mass flow rate within a simulated salted egg curing vessel at 404 kPa and 60°C.

The technical implications of this data are emphasized to minimize fluid motion to facilitate consistent curing. The initial instability suggests potential challenges in establishing a stable flow regime, which requires design considerations to mitigate transient flows, such as optimizing inlet and outlet configurations and gradual heating protocols. Furthermore, the converged near-zero mass flow rate emphasizes the importance of maintaining a static environment through uniform heating, effective insulation, and the minimization of external disturbances. This data serves as a validation of the reliability of the simulation and highlights the significance of operating conditions in establishing a diffusion-driven curing process that contributes to the development of optimized vessel designs for high-quality salted egg production.

3.5.2. Velocity field stability and flow uniformity

The convergence behavior of average velocity within a simulated salted egg curing vessel at 404 kPa and 60°C was illustrated in Figure 4. The average velocity decreases rapidly from 0.12 m/s to 0.04 m/s within the initial 100 iterations and eventually stabilizes at approximately 0.01 m/s by the 500th iteration, which confirms the establishment of a near-quiescent environment. The low-velocity fields strengthen a diffusion-controlled curing process, which is consistent with findings from Gómez et al. [11] who emphasize the need for thermal uniformity and minimal turbulence in curing systems.

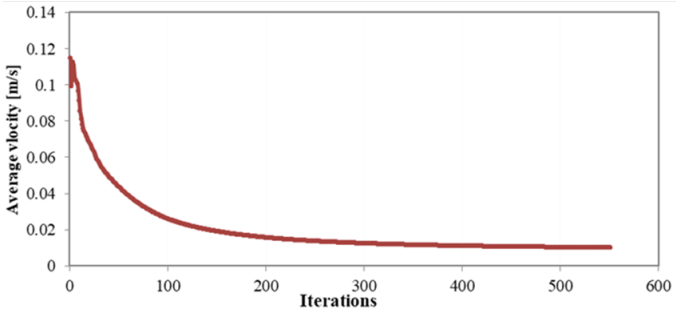

Figure 4. The convergence behavior of average velocity within a simulated salted egg curing vessel at 404 kPa and 60°C.

This trend signifies the establishment of a near-quiescent environment where fluid motion is minimal and indicates that the curing process is predominantly diffusion-driven. The convergence to a low and stable velocity value signifies the importance of maintaining a static environment in the curing vessel to facilitate uniform salt penetration. The design should prioritize features that minimize fluid movement, such as optimized geometry, uniform heating, and adequate insulation, to ensure consistent curing. The convergence also validates the reliability of the CFD simulation and provides valuable insights for design optimization, highlighting the significance of operating conditions in achieving a diffusion-dominated curing process.

The maximum local velocity of 3.74 m/s, although isolated from the graph and can be seen in Table 5, indicates the presence of narrow channels or localized flow paths where geometry may induce temporary acceleration. These findings allow future geometric refinement to further suppress localized flow intensification and minimize any possibilities for convective effects.

Table 5. Summary of flow simulation parameter

Goal	Unit	Value	Average	Minimum	Maximum	Delta	Criteria
Mass flow rate	[kg/s]	-0.0004	-0.0002	-0.0012	0.0005	0.00007	0.725
Minimum total pressure	[Pa]	401111.36	401136.11	401087.38	401197.15	5.1035	2480.218
Average total pressure	[Pa]	404001.70	404001.71	404001.68	404001.76	0.0719	483.015
Maximum total pressure	[Pa]	410175.30	410064.26	409946.85	410205.97	10.563	7364.825
Minimum fluid temperature	[K]	293.13	293.13	293.13	293.13	0.00047	0.0041
Average fluid temperature	[K]	313.36	313.11	312.81	313.36	0.5515	0.553
Maximum fluid temperature	[K]	353.20	353.20	353.20	353.20	0.0014	0.029
Mass flow rate	[kg/s]	-0.0004	-0.0002	-0.0012	0.0005	0.00007	0.725
Minimum velocity	[m/s]	0.0000	0.0000	0.0000	0.0000	0.00000	0.000
Average velocity	[m/s]	0.0100	0.0104	0.0100	0.0108	0.00086	0.00299
Maximum velocity	[m/s]	3.74	3.73	3.73	3.75	0.00056	0.14207

The analysis of convergence metrics obtained from CFD simulation of a salted egg curing vessel focused on the critical parameters that influence the curing process. The simulation aimed to evaluate the performance of the vessel by monitoring mass flow rate, pressure distribution, temperature profiles, and velocity fields. The convergence data are all within the 500 iterations, which demonstrates a stable numerical solution, evidenced by the achievement of 100% convergence across all monitored goals. The statistical behavior of the simulation outputs further confirms reliability. The narrow variation ranges observed in Table 5, such as the ±0.00007 kg/s deviation in mass flow rate, the ±0.00299 m/s variation in average velocity, and the ≤10.56 Pa spread in total pressure is an indication of a highly stable numerical solution with minimal iteration-to-iteration variability. These low delta values function as statistical indicators that the computed fields are consistent and reproducible, which strengthens the applicability of the CFD results to real curing conditions.

3.5.3. Pressure and temperature distribution

Pressure distribution remains tightly clustered around 404 kPa as presented in Figure 5(a). The minimum pressure, average pressure, and maximum total pressures have a narrow spread and a maximum variation of only ~10.56 Pa as reflected in Table 5. This uniformity indicates a stable pressure field and a minimal potential inconsistency in salt uptake due to pressure [9,10]. This stability contrasts significantly with ultrasonic-pulsed curing systems documented by Wang et al. [2], which demonstrated large transient pressure fluctuations that may impede uniform curing.

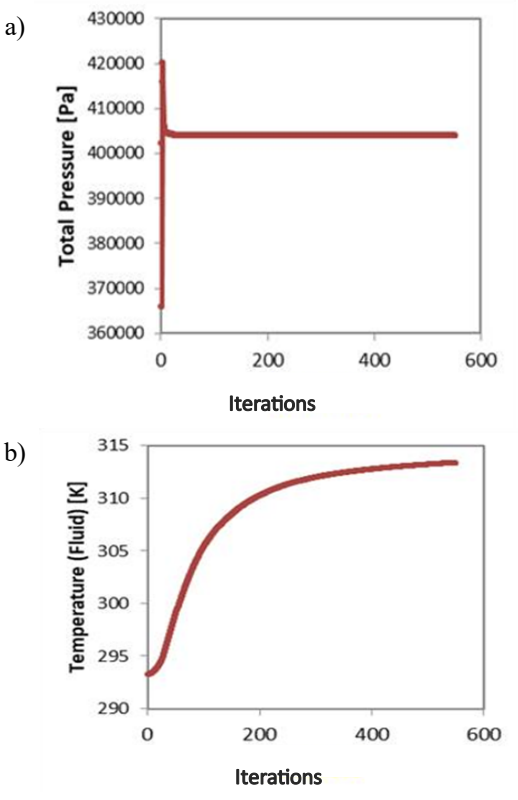

Figure 5. (a) The convergence behavior of (a) total pressure, (b) temperature of the fluid within a simulated salted egg curing vessel at 404 kPa and 60°C.

Thermal distribution is likewise consistent, as presented in Figure 5(b), with fluid temperatures ranging from 293 K to 353 K. An average temperature of 313 K highlights the necessity for precise thermal management to ensure uniform curing kinetics [11]. The uniformity of the thermal field is largely attributed to the vessel's cylindrical geometry and optimized thermal load application that supports a consistent curing kinetics throughout the volume.

3.5.4. Flow trajectories and recirculation patterns

The image in Figure 6 depicts a snapshot of a time-dependent CFD simulation of fluid flow within a complex vessel at approximately 26 s of simulation. It highlights the spatial distribution of fluid motion under the imposed pressure and thermal conditions. The primary visual element is the representation of fluid flow through green lines and depicting flow trajectories that reveal a dynamic movement pattern within the vessel. These trajectories show a combination of directional flow and swirling motions that indicate potential turbulence and mixing that is crucial for ensuring uniform processing within the vessel [12]. The pressure scale on the left that ranges from 401146.79 Pa to 407636.32 Pa suggests that a pressure gradient is driving the flow and has higher pressure regions that correspond to inlet zones and lower pressure regions to outlet zones. The "Flow Trajectories 1" label indicates that this is one representation of the flow and potentially part of a series or highlights a specific aspect of the flow behavior.

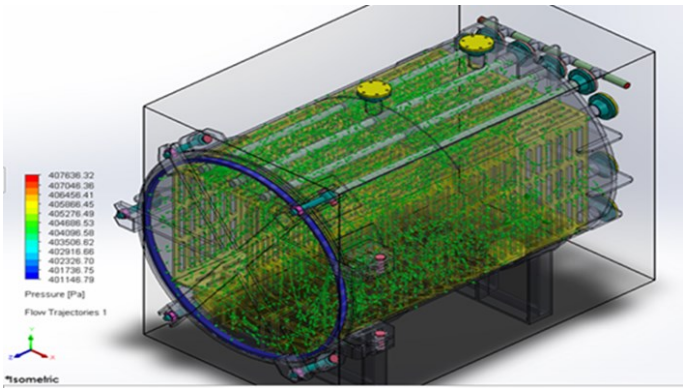

Figure 6. The visual presentation of the flow simulation of the curing vessel.

Compared to stirred-tank reactors where intensive circulation loops and high turbulence zones are intentionally promoted [12,13], the present vessel exhibits markedly lower turbulence intensity and smaller recirculation structures. This distinction is critical in the design of rapid curing of salted eggs but controlled diffusion under relatively quiescent conditions. In this context, the modest recirculation zones observed can be interpreted as beneficial for smoothing local concentration and temperature gradients without generating large-scale convective transport that would compromise diffusion-dominated curing.

These flow patterns also have implications for internal design features such as baffle placement, nozzle orientation, and internal racks or the baskets used for egg loading. Areas of higher streamline density could guide future reinforcement or geometric smoothing, while regions with sparse

trajectories may identify potential stagnation zones that warrant minor design adjustments. Overall, the design complements the convergence and velocity data by providing spatial confirmation that the internal flow regime remains consistent with the intended diffusion-driven curing mechanism.

Similarly, pressure-assisted curing systems using ultrasonic–pulsed pressure technology, such as those described by Wang et al. [2], exhibited strong transient fluctuations in internal pressure and velocity fields. These fluctuations may compromise curing uniformity. The current vessel, in comparison, sustains extremely stable pressure conditions with only ~10.56 Pa variation across the domain during the 5-day simulated curing cycle. This stability reflects an improvement over pulsed-pressure systems and supports consistent diffusion-controlled curing. Thermal distribution comparisons also demonstrate the strength of the present design. Prior food-curing simulations in Gómez et al. [11] reported temperature gradients due to uneven heating. The proposed vessel achieves a uniform temperature distribution within ±1°C of the setpoint that is attributed to its cylindrical geometry and optimized thermal loading. This thermal uniformity is critical in controlling curing kinetics and is superior to earlier thermally driven curing systems. While previous studies examined individual aspects of the designs, such as mixing behavior, pulsed pressure curing or thermal diffusion, the current study integrates structural integrity, fluid flow, thermal behavior, and corrosion resistance into a single multi-physics simulation. This comprehensive approach has not been previously applied to salted-egg curing vessels and represents a significant contribution to food engineering and pressure-vessel design.

The attainment of 100% convergence across all goals, coupled with minimal delta values, confirms the numerical stability and reliability of the simulation. These findings have significant implications for the design and optimization of salted egg curing vessels. Specifically, the low mass flow rate and velocity fields necessitate design considerations that minimize forced convection and ensure a diffusion-driven process. The uniform pressure distribution emphasizes the importance of minimizing pressure gradients to maintain consistent curing. Furthermore, the temperature profiles emphasize the need for robust thermal control systems to achieve and maintain the desired curing temperature. The convergence data presented in this study provide valuable insights into fluid dynamics and heat transfer within the curing process and facilitate the development of optimized designs for consistent and high-quality salted egg production.

Technically, this simulation offers valuable insights into the design of the vessel. The flow trajectories reveal areas of high and low velocity, which can be used to optimize the placement and design of internal components to enhance mixing and ensure uniform processing. The concentrated flow lines could indicate areas of high velocity and high potential for corrosion that need material reinforcement. On the contrary, regions with thin flow lines might signify stagnation, affecting the processing efficiency that leads to localized over-processing or under-processing.

The system requirement for hydraulic behavior is based on the simulated pressure, which is the basis for the accurate specification of the capacity of the fluid to flow in maintaining stable operating pressures and adequate brine circulation. Moreover, the complex internal flow geometry visible in the simulation facilitates evaluation of engineering decisions such as baffle spacing, nozzle orientation, and pipe diameter selection that ensure these elements achieve the targeted flow distribution. The swirling patterns observed in the flow trajectories suggest potential areas of enhanced mixing, which could be beneficial for ensuring uniform heat distribution or chemical activity during the processing. The simulation also highlights the importance of considering the pressure drop across the vessel because it directly impacts the energy required to maintain the desired flow rate that may affect operational efficiency. Ultimately, this CFD serves as a robust computational basis for refining the vessel architecture while enabling a design to satisfy performance specifications, mitigating flow-induced risks, and enhancing operational efficiency within the intended processing environment.

4. Conclusions

This study addressed the challenge of developing a rapid, hygienic curing vessel for continuous salted-egg production that can operate under high pressure, controlled thermal conditions, and a highly saline and acidic environment. A simulation-driven design framework that used FEA and CFD modelling was used to evaluate the structural integrity, internal flow regime, thermal stability, and corrosion resistance capacity of a high-capacity vessel that is fabricated using AISI 1020 steel with food-grade protective linings. The numerical outcomes indicate that the proposed design satisfies the mechanical, thermal, and process requirements for a diffusion-dominated curing process. Likewise, it also incorporates measures to mitigate the long-term corrosion and product contamination risks. The study also demonstrates the effectiveness of multi-physics simulation as a design and screening tool for pressure-assisted food processing equipment that operates in a chemically aggressive environment. While the findings establish technical feasibility at the design stage, future works should focus on experimental validation with the prototype fabrication and testing, transient thermo-mechanical analysis, and assessment of long-term corrosion performance to support industrial implementation and regulatory compliance.

Acknowledgment

The authors extend their gratitude to the Philippine Council for Industry, Energy, and Emerging Technology Research and Development of the Department of Science and Technology (DOST-PCIEERD) for supporting this project.

References

[1] Kasler DR, Pyatkovskyy T, Yousef AE, Sastry SK. Effect of moderate electric field pretreatment in combination with ozonation on inactivation of Escherichia coli K12 in intact shell eggs. LWT [Internet]. 2020 Jun;127:109338. Available from: https://doi.org/10.1016/j.lwt.2020.109338

[2] Wang S, Zhang Y, Zhang R. Parameter optimization for quickly salted egg by using ultrasonic-pulsed pressure technology. Nongye Gongcheng Xuebao Trans Chin Soc Agric Eng [Internet]. 2013 Dec;29(23):286-92. Available from:https://doi.org/10.3969/j.issn.1002

6819.2013.23.039
[3] Schweitzer PA. Corrosion-resistant linings and coatings [Internet]. Boca Raton: Taylor & Francis Group; 2001. 448 p. Available from: https://doi.org/10.1201/9781482270891
[4] Khanna AS. High-performance organic coatings [Internet]. Cambridge, United Kingdom: Woodhead Publishing Limited; 2008. 472 p. Available from: https://doi.org/10.1533/9781845694739
[5] Jotun protects property | [DE] [Internet]. Jotun protects property; [date unknown]. Available from: https://www.jotun.com/ww-en
[6] Dang TN, Tao AT. Research on the effect of welding parameters on tensile properties of dissimilar base materials (low carbon steel AISI 1020 and stainless steel AISI 304) rotary friction welding joint using Taguchi method. J Tech Educ Sci (J Tech Educ Sci) [Internet]. 2018;13(6):25-33. Available from: https://jte.edu.vn/index.php/jte/article/view/278
[7] Code of Federal Regulations [Internet]. CFR title 21 §175.300 - resinous and polymeric coatings [internet].; [date unknown]. Available from: https://www.ecfr.gov/current/title-21/chapter-I/subchapter-B/part-175/subpart-C/section-175.300
[8] EHEDG: Food safety, quality, productivity, sustainability | EHEDG [Internet]. EHEDG: guideline catalogue; [date unknown]. Available from: https://www.ehedg.org/guidelines
[9] Tartakovsky DM, Dentz M. Diffusion in porous media: phenomena and mechanisms. Transp Porous Media [Internet]. 2019 Mar 18;130(1):105-27. Available from: https://doi.org/10.1007/s11242-019-01262-6
[10] Li C, Shi J, Zhai X, Yang Z, Huang X, Li Z, Li Y, Zou X. Effects of pulsed pressure curing on beef quality. Foods [Internet]. 2023 Feb 3;12(3):656. Available from: https://doi.org/10.3390/foods12030656
[11] Gómez J, Sanjuán N, Bon J, Arnau J, Clemente G. Effect of temperature on nitrite and water diffusion in pork meat. J Food Eng [Internet]. 2015 Mar;149:188-94. Available from: https://doi.org/10.1016/j.jfoodeng.2014.10.008
[12] Qu W, Xie H, Wang H, Xiong J. Experimental study of turbulent flow in lower plenum with flow skirt of reactor pressure vessel of pressurized water reactor. Ann Nucl Energy [Internet]. 2024 Jun;201:110440. Available from: https://doi.org/10.1016/j.anucene.2024.110440
[13] Kumaresan T, Nere NK, Joshi JB. Effect of internals on the flow pattern and mixing in stirred tanks. Ind & Eng Chem Res [Internet]. 2005 Dec;44(26):9951-61. Available from: https://doi.org/10.1021/ie0503848